

See discussions, stats, and author profiles for this publication at: <https://www.researchgate.net/publication/230642005>

Formation and Characterization of Long-Lived Negative Molecular Ions of C₆₀H₁₈

ARTICLE in THE JOURNAL OF PHYSICAL CHEMISTRY A · FEBRUARY 2001

Impact Factor: 2.69 · DOI: 10.1021/jp002890a

CITATIONS

20

READS

18

6 AUTHORS, INCLUDING:



Yury V Vasil'ev

Oregon State University

35 PUBLICATIONS 566 CITATIONS

SEE PROFILE



Rinat Abzalimov

City College of New York

33 PUBLICATIONS 768 CITATIONS

SEE PROFILE

LETTERS

Formation and Characterization of Long-Lived Negative Molecular Ions of C₆₀H₁₈

Yury V. Vasil'ev,^{†,‡} Rinat R. Absalimov,[‡] Shamil' K. Nasibullaev,[‡] Anatolii S. Lobach,[§] and Thomas Drewello^{*,†}

*Department of Chemistry, University of Warwick, Coventry CV4 7AL, England, U.K.,
Institute of Physics of Molecules and Crystals, Ufa Research Centre, Russian Academy of Sciences,
450075, Ufa, Russia, and Institute of Problems of Chemical Physics, Russian Academy of Sciences,
142432 Chernogolovka, Moscow Region, Russia*

Received: August 10, 2000; In Final Form: November 16, 2000

Long-lived molecular negative ions are generated from C₆₀H₁₈ following the application of several ionization methods such as laser desorption/ionization, negative ion chemical ionization, and resonant free electron capture. The mass spectrometric observation of stable negative fullerene ions showing such a high degree of hydrogen attainment is unprecedented. The identity of the negative molecular ion is confirmed by high-resolution accurate mass measurements. The attachment of monochromatic electrons to C₆₀H₁₈ is studied in the energy range from 0 to 20 eV, and the resulting negative ion effective yield curve is discussed together with the mean lifetime curve of the ion. Negative molecular ions that result from capture of thermal electrons at a molecular temperature of 600 K possess a maximum mean lifetime in the range of 1 ms. From the experimental data the electron affinity of C₆₀H₁₈ is estimated to lie between 1.4 and 1.6 eV, which is in excellent agreement with the results obtained here from semiempirical calculations.

Introduction

Hydrogenated fullerenes are commonly referred to as the first ever fullerene derivatives to be synthesized. The hydrogenation of fullerenes is readily achieved by a variety of synthetic methods including the Birch reduction,¹ hydrogen transfer reduction,^{2,3} catalytic hydrogenation,⁴ and Zn/HCl reduction.⁵ C₆₀H₃₆ and C₆₀H₁₈ are the most prominent representatives of this class of compounds. Although the research into hydrogenated fullerenes has continued for over a decade, the structure elucidation is of such a complexity that only very recently has

major progress been made in the assignment of the geometries of C₆₀H₃₆ and C₆₀H₁₈.⁶ Throughout this period, mass spectrometry-based experiments have been of tremendous importance as the essential tool for the product analysis. Besides ion fragmentation, the major complication for the unambiguous product analysis of hydrogenated fullerenes arises from thermal decomposition of the sample, resulting in extensive liberation of the attached hydrogen. Only a few ionization methods, such as field desorption,² matrix-assisted laser desorption^{7,8} and, to some extent, desorption electron ionization⁵ were found to be sufficiently free of fragmentation resulting in cationic species, being indicative of the neutral precursor. Even more dramatic is the situation for anionic hydrofullerenes. In striking contrast to their fluorinated counterparts, which are believed to possess similar, if not identical, structural features⁶ and which readily form long-lived molecular anions at any degree of fluorination,^{9,10} the hydrogenated fullerenes are currently believed to

* Corresponding author. Fax: +44-2476-524112. E-mail: t.drewello@warwick.ac.uk.

[†] University of Warwick.

[‡] Institute of Physics of Molecules and Crystals, Russian Academy of Sciences.

[§] Institute of Problems of Chemical Physics, Russian Academy of Sciences.

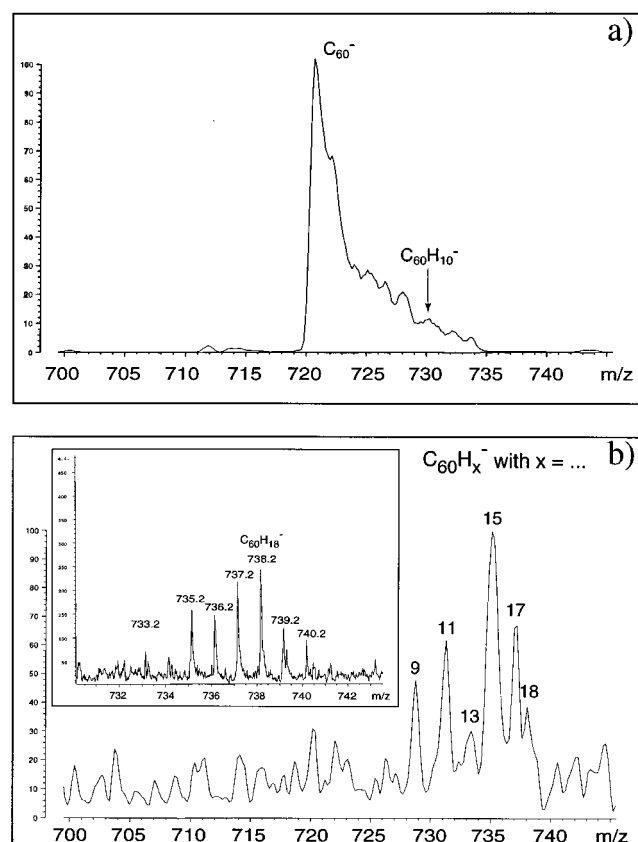


Figure 1. Negative ion laser desorption/ionization ToF mass spectra of $C_{60}H_{36}$ (a) and $C_{60}H_{18}$ (b) recorded at the threshold of the ion formation. The inset in (b) was recorded at higher mass resolving power.

form mass spectrometrically observable negative ions only up to an attachment of 10 hydrogen atoms to the C_{60} cage.^{11,12} In pioneering laser desorption/ionization experiments on $C_{60}H_{36}$, the most abundantly formed anion was $C_{60}^{\bullet-}$ accompanied by anionic hydrofullerenes of decreasing abundance where $C_{60}H_{10}^{\bullet-}$ was the ion with the highest hydrogen attainment.^{11,12} These findings have been related to theoretical considerations according to which the electron affinity monotonically decreases with increasing hydrogen content, showing the most pronounced decline at around $C_{60}H_{10}$. However, based on these semiempirical calculations and employing Koopman's theorem, stable negative molecular ions can still be expected for hydrogenated [60]fullerenes with more than 20 hydrogen atoms.^{13,14} For a hydrogen attainment in the order of 30–40 hydrogen atoms, the electron affinity is expected to become negative in magnitude, making the observation of the corresponding negative ions unlikely. Preliminary experiments based on resonant electron capture mass spectrometry have provided indications for the possible existence of the long-lived molecular negative ion of $C_{60}H_{18}^{\bullet-}$; however, the elemental composition of this ion could not be established unambiguously.¹⁵ Following our recent investigations into the fragmentation¹⁶ and ionization dynamics of hydrogenated C_{60} ,⁸ we report here on the unprecedented finding of long-lived, negative molecular ions derived from $C_{60}H_{18}$.

A comparison of the negative ions derived from laser desorption/ionization is made using $C_{60}H_{36}$ and $C_{60}H_{18}$ as the target materials for ablation. The identity of the $C_{60}H_{18}^{\bullet-}$ anion is established by high-resolution accurate mass measurements following secondary electron capture of $C_{60}H_{18}$ in negative ion chemical ionization experiments. Utilizing a monochromatic

electron beam in an energy range from 0 to 20 eV, the resonant free electron capture behavior of $C_{60}H_{18}$ is recorded. The resulting negative ion effective yield curve and the mean lifetime curve of $C_{60}H_{18}^{\bullet-}$ as functions of the electron energy are discussed. Based on the negative ion mean lifetime, the Arrhenius plot of the electron autodetachment rate constant as a function of the inverse molecular temperature enables an estimation of the adiabatic electron affinity of the $C_{60}H_{18}$ molecule.

Experimental Section

Laser desorption/ionization was accomplished by the use of a curved-field reflectron time-of-flight (ToF) mass spectrometer (Kratos Kompact MALDI IV, Kratos Inc., Manchester, UK) which has recently been applied to a variety of fullerene-related investigations.^{8,10,16–18} The instrument operates a nitrogen laser (at 337 nm, 3 ns pulse width) and applies a continuous acceleration voltage of 20 kV. Each individual ToF mass spectrum shown represents the accumulation of 200 single-laser-shot spectra. The resolution was below 1000. The samples were deposited on a stainless steel slide as THF solutions at a 1 mg/mL concentration and dried in an air stream preceding the insertion into the ion source of the mass spectrometer. For a more accurate assignment in the mass range of interest a reflectron ToF mass spectrometer of higher resolving power (Bruker Reflex, Bruker, Coventry, UK) was employed and the data are shown as the insert in Figure 1b.

The accurate mass measurements were performed using a sector instrument (AutoSpec, Micromass Ltd., Altrincham, UK) of EBE geometry (E stands for the electric sector and B denotes the magnetic sector). The sample was evaporated from a heated solid probe tip, and the resolution in these experiments was greater than 6000. For full negative ion mass spectra, the sample was desorbed from a desorption chemical ionization (DCI) probe tip by heating. In both of these approaches the negative ions were derived from bombardment of the gaseous sample with 20 eV electrons, employing ammonia as a buffer gas.

Resonant electron capture mass spectra including the recording of the effective yield curves of the negative ions and the determination of their mean lifetimes were performed utilizing a single focusing magnetic sector mass spectrometer (MI-1201, Russia). This instrument is equipped with a homemade trochoidal electron monochromator (TEM) for the generation of the monochromatic electron beam.¹⁹ The electron energy spread was $\Delta\epsilon = 200\text{--}250$ meV in the present experiments. A better energy resolution was prevented by the low abundance of the ions derived from hydrogenated fullerenes. A molecular beam was created by heating of hydrofullerene samples in an oven at a temperature of ca. 350 °C. The pressure, measured by an ion gauge located close to the ionization chamber, was not higher than $10^{-8}\text{--}10^{-9}$ Torr; this pressure corresponds to single-collision conditions within the source. The electron energy scale was calibrated using the maxima of the effective yield curves of $SF_6^{\bullet-}$ (≈ 0 eV) and $NH_2^{\bullet-}$ from NH_3 (5.65 eV). The determination of the mean lifetime of the negative ions has been achieved as described in ref 19.

$C_{60}H_{18}$ and $C_{60}H_{36}$ were synthesized as reported in the literature by transfer hydrogenation from dihydroanthracene.³

Results and Discussion

The negative ion LDI mass spectra of $C_{60}H_{36}$ and $C_{60}H_{18}$ are shown in Figure 1, a and b, respectively. Both spectra have been obtained at laser fluences closely adjusted to the threshold of the ion formation. The appearance of the spectrum derived

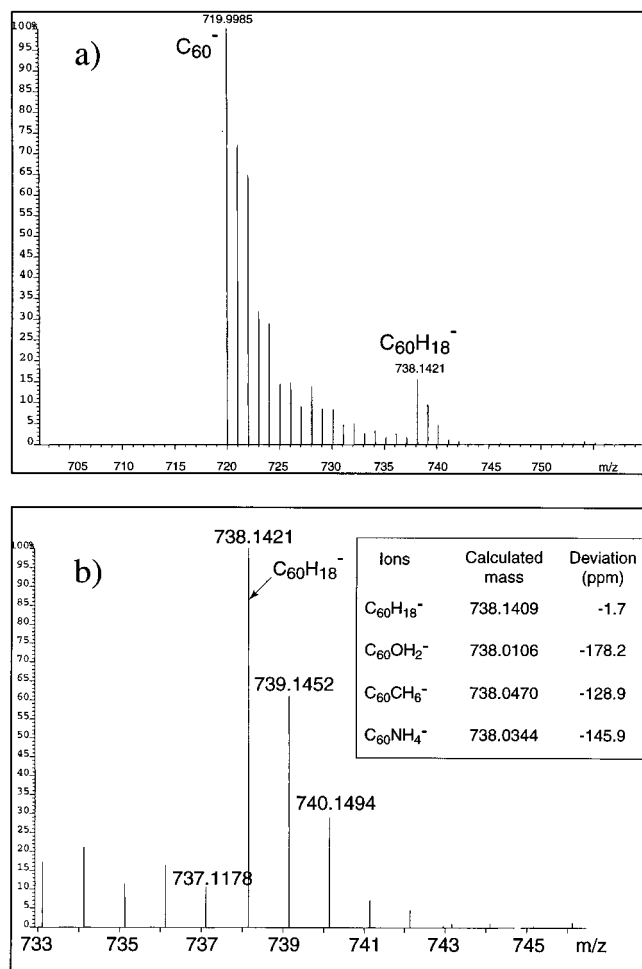


Figure 2. (a) Negative ion chemical ionization mass spectrum of $C_{60}H_{18}$ (20 eV, ammonia as buffer gas) in the mass range of 700–760 Da recorded with a sector mass spectrometer. (b) Expanded molecular ion region of (a) with the measured accurate masses. The inset in (b) provides the calculated masses for different ions of m/z 738 and their deviation (in ppm) from the experimentally determined value of 738.1421 Da.

from $C_{60}H_{36}$ shows a close resemblance to the data reported earlier.^{11,12} Following the C_{60}^- base peak, the spectrum is characterized by a rapidly descending abundance of hydrofullerene ions. In striking contrast, the laser ablation of the $C_{60}H_{18}$ target leads to the abundant formation of $C_{60}H_x^-$ ions with x being well above 10 hydrogen atoms, the previously assumed upper limit for stable negative ions of the hydrogenated [60]-fullerene. The insert in Figure 1b shows the molecular ion region with a sufficiently high resolving power to enable the distinction between individual signals of different nominal masses. The negative molecular ion of $C_{60}H_{18}$ is clearly observed and accompanied by several signals from negative ions of lower hydrogen content derived by fragmentation. The differences between the observed mass distributions, obtained in both of the LDI experiments (Figure 1b and insert), results from the differing threshold laser fluences required for ion formation. Both samples investigated here contained trace amounts of anthracene caused by the use of dihydroanthracene for the transfer reduction of C_{60} . Although it cannot be excluded that the anthracene might have a matrix-like effect in these desorption experiments, the fact, however, that both samples are investigated under identical conditions allows a direct comparison. As the resolving power in the LDI experiments is insufficient to confirm the assumed elemental composition of

the ion observed and due to unavailability of 2H -labeled target material, which would lead to a mass shift of 1 Da per incorporated 2H atom, accurate mass measurements were performed using a higher resolving sector instrument and applying negative ion chemical ionization. The resulting spectrum is depicted in Figure 2. Using ammonia as the buffer gas, $C_{60}H_{18}$ is desorbed from a heated DCI-probe tip (ca. 350 °C) into a nonmonochromatic 20 eV electron beam, resulting in the formation of negative ions via attachment of thermalized secondary electrons. The mass resolving power of 6000 is sufficient to separate $C_{60}H_{18}^-$ from potentially interfering ions of the same nominal mass, which are listed in the inserted table (Figure 2b). Following the initial mass calibration with PFK, the C_{60}^- signal at m/z 720 is used as an internal calibrant, leading to the determination that the ions with a nominal m/z 738 had an accurate mass value of 738.1421, which is 1.7 ppm higher than the calculated mass $C_{60}H_{18}^-$. This experiment confirms the $C_{60}H_{18}^-$ identity as the other listed elemental compositions would lead to significantly larger deviations (Figure 2b). From Figure 2b it is also evident that the $C_{60}H_{18}^-$ signal is enhanced when compared to neighboring ions of lower hydrogen content, so that contributions due to ^{13}C isotopomers for these ions are of minor importance. Moreover, the analysis of the ^{13}C contributions to the various signals shown in Figure 2 reveals that only negative ions which possess an even number of hydrogen atoms are efficiently formed. In addition to $C_{60}H^-$, which is formed with an intensity of approximately 5% relative to C_{60}^- , the abundances of species of higher odd hydrogen content remained indistinguishable from the expected intensities of the ^{13}C isotopomers of species of even hydrogen content. The reduced formation of odd-numbered species under DCI conditions can be rationalized as follows. Neutral fragments of even hydrogen content are initially formed by thermal dehydrogenation of $C_{60}H_{18}$, followed by the capture of electrons that are thermalized by collisions with the buffer gas. The efficient decay of these ions into fragment ions of odd hydrogen content is prevented in this low-energy process. The observation of abundant odd numbered species under LDI conditions (Figure 1b) indicates that the energy distribution of the captured electrons is wider, clearly also covering higher energies.

While $C_{60}H_{18}^-$ is thus a perfectly stable species, it undoubtedly escapes experimental observation when LDI is applied to $C_{60}H_{36}$ as the target material. This is probably a consequence of the mode of sample activation rather than a reflection of the stability of this ion. In this context, an interesting comparison can be drawn to cationic species. The EI mass spectrum of pure $C_{60}H_{36}$ frequently comprises the $C_{60}H_{18}^{+\bullet}$ signal as one of the most prominent features, clearly indicating its pronounced formation in the course of the analysis. Applying tandem mass spectrometry, we have recently shown¹⁶ that $C_{60}H_{18}^{+\bullet}$ cations are generated in only minor amounts through the fragmentation of cationic $C_{60}H_{36}^{+\bullet}$, which undergoes cage breakage in competition to the loss of hydrogen. $C_{60}H_{18}^{+\bullet}$ cations are thus predominantly formed via the decomposition of neutral $C_{60}H_{36}$ caused by thermal excitation (heating) preceding the ionization. In contrast, applying laser ablation, no significant enhancement of the $C_{60}H_{18}^{+\bullet}$ signal is evident from numerous investigations into the formation of positive ions from pure $C_{60}H_{36}$ targets,^{8,16,20,21} even though $C_{60}^{+\bullet}$ could be observed, indicating that efficient fragmentation takes effect. It seems therefore reasonable to assume that laser ablation of $C_{60}H_{36}$ fails to produce a sufficient amount of $C_{60}H_{18}$ in the neutral stage to allow the subsequent ionization, which explains the lack of

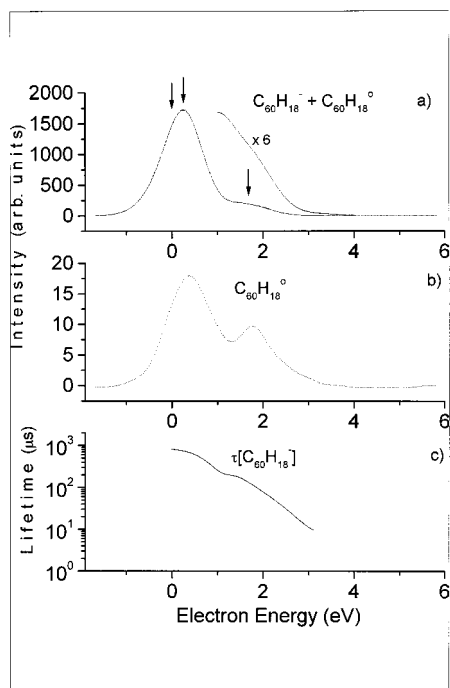


Figure 3. (a) Experimental effective yield curve (dotted line) of the total current including negative ions, $C_{60}H_{18}^{\bullet-}$, and neutrals, $C_{60}H_{18}^0$ (which are formed by electron autodetachment from the negative ions), as a function of the electron energy. Three Gaussian-shaped curves (not shown) centered at 0, 0.3, and 1.7 eV were added to fit the data (solid line). The arrows indicate the electron energies of 0, 0.3, and 1.7 eV. (b) The current of neutral $C_{60}H_{18}^0$ as a function of the electron energy. (c) The mean lifetime of $C_{60}H_{18}^{\bullet-}$ negative ions as a function of electron energy after subtraction of the plateaulike behavior of the curve observed at the high-energy side (see text).

$C_{60}H_{18}^{\bullet-}$ anions in the negative ion LDI mass spectrum of $C_{60}H_{36}$ (Figure 1a).

Following the establishment of stable molecular negative ions of $C_{60}H_{18}$, the process of electron attachment to $C_{60}H_{18}$ is studied in more detail to gain insight into ion yields and the lifetime magnitude as a function of electron energy. For this purpose $C_{60}H_{18}$ was evaporated from an oven (350 °C) and crossed with a beam of monochromatic electrons covering an energy range of 0–20 eV. Negative ions derived from the direct, resonant capture of these monoenergetic electrons were analyzed employing a single focusing magnetic sector mass spectrometer. The resulting ion yield curve is shown in Figure 3a, featuring a rise in ion abundance at around 0 eV and showing two broad resonances centered at approximately 0.3 and 1.7 eV, followed by a smooth decline of the ion abundance at ca. 3.5 eV. In striking contrast to the declining ion abundance between 2 and 3.5 eV observed in the present case, the negative ion formation of unsubstituted C_{60} extends far beyond this energy up to an upper limit of about 14 eV.^{19,22–25} Hydrogenation thus reduces the energy range in which long-lived molecular ions can result from electron capture. However, the observed features reflect still very clearly the unique characteristics of the fullerene core, especially when considering that prior to the advent of the fullerenes, only two examples were reported for the formation of long-lived polyatomic, molecular negative ions at electron energies as high as in the present case.^{26,27}

The capture of s-electrons at 0 eV is characterized by a relatively low cross section, while the capture of electrons with energies centered around 0.3 eV is clearly the most pronounced process followed by the enhanced electron capture at around 1.7 eV. The observation that the thermal resonance at 0 eV is

characterized by a lower abundance, when compared to the feature centered at approximately 0.3 eV, is not surprising for the electron attachment to fullerene-based materials. Earlier beam experiments including C_{60} ^{19,22–25} and fluorofullerenes⁹ have shown very similar features. This behavior might indicate that the ground state of the molecular negative ions is not fully symmetric, so that the excitation of vibrational modes is required to satisfy the symmetry rules during the electron capture event. Prior to the discovery of fullerenes, only a few exceptional cases had been reported showing a similar cross section behavior.²⁸ In all these cases, the mean ion lifetime at the thermal resonance exceeded the lifetime of the ions generated at resonances of higher energies.

The abundances shown in Figure 3a are obtained by a detector that responds to the impact of all forward moving particles. In addition to the magnet-selected negative ions of interest, contributions to the resulting yield curve of detected particles (Figure 3a) can also be caused by neutrals that are formed from the selected anions. Under the present experimental conditions, the most likely origin of neutrals in the particle beam is through electron autodetachment from negative ions. The low pressure in these experiments means that contributions caused by collision-induced neutralization can be discounted. The neutrals resulting from electron autodetachment can be detected in the present setup following the orthogonal deflection of ions from the beam. The resulting neutral yield curve is depicted in Figure 3b. The data clearly reveal the enhanced formation of neutrals with maxima at slightly higher energies (0.38 and 1.9 eV) than seen in the total yield curve (Figure 3a), which reflects the decreasing ion lifetime within these resonances as the electron energy is increased. The relative ratio of neutrals to ions is larger for the high-energy resonance at 1.7 eV, indicating a larger rate for the autodetachment of electrons from this resonant state. From the data shown in Figure 3a,b the abundance of ions can be distinguished from the abundance of neutrals at a known flight time. Assuming an exponential decay of the negative ion via electron autodetachment, these findings allow the establishment of the mean ion lifetime of the $C_{60}H_{18}^{\bullet-}$ ion as a function of the kinetic energy of the initially captured electron. The negative ion lifetime curve for $C_{60}H_{18}^{\bullet-}$ is depicted as Figure 3c. At 0 eV the ion lifetime amounts to approximately 820 μs and declines to about 10 μs at 3 eV.

The electron affinity of $C_{60}H_{18}$ has been determined from the slope of an Arrhenius plot correlating the electron autodetachment rate constant as derived from the ion lifetime measurements and the inverse vibrational temperature of the molecule. The molecular vibrational temperature has been determined using the Boltzmann population distribution and vibrational frequencies calculated for $C_{60}H_{18}$ of C_{3v} symmetry by MNDO. The data were modified as in the case of C_{60} ²⁹ in order to reproduce experimental values.³⁰ Depending on the subtraction procedure for the plateaulike part of the lifetime curve of $C_{60}H_{18}^{\bullet-}$ observed at high energies, the electron affinity of $C_{60}H_{18}$ has been found to range between 1.4 and 1.6 eV. Applying MNDO and Koopman's theorem, the electron affinities of all possible isomers possessing a C_3 symmetry axis have been determined. In agreement with the experimental data, it has been found that the electron affinity of all these isomers is positive in magnitude ranging from 1.13 to 1.79 eV. Furthermore, when the obtained lifetime values are converted to electron autodetachment rate constants, a comparison can be made with the theoretical rate constants derived from a thermionic emission model.³¹ By taking the internal energy and a degeneracy factor of 4 for the C_{3v} isomer into account, a value

of 1.6 eV for the electron affinity leads to good agreement of the experimental and theoretical rate constants. This is in striking contrast to C_{60}^{*-} , for which the discrepancy is known to be substantial.³² A more elaborate account on these considerations and on the method of the electron affinity determination, together with the details of the theoretical data on different neutral $C_{60}H_{18}$ isomers and their corresponding negative ions, will be published in a forthcoming paper.³³

Acknowledgment. We are thankful to Inder Katyal for his skillful assistance during the accurate mass measurements and to Dr. J. A. Jarvis (Bruker, Coventry) for her help in obtaining the data shown as insert in Figure 1b. Support of our work by the Russian Foundation for Basic Research, INTAS, and the Leverhulme Trust (England) is gratefully acknowledged.

References and Notes

- (1) Haufler, R. E.; Conceicao, J.; Chibante, L. P. F.; Chai, Y.; Byrne, N. E.; Flanagan, S.; Haley, M. M.; O'Brien, S. C.; Pan, C.; Xiao, Z.; Billups, W. E.; Ciufolini, M. A.; Hauge, R. H.; Margrave, J. L.; Wilson, L. J.; Crul, R. F.; Smalley, R. E. *J. Phys. Chem.* **1990**, *94*, 8634.
- (2) Rückhardt, C.; Gerst, M.; Ebenhoch, J.; Beckhaus, H.-D.; Campbell, E. E. B.; Tellmann, R.; Schwarz, H.; Weiske, T.; Pitter, S. *Angew. Chem., Int. Ed. Engl.* **1993**, *32*, 584.
- (3) Lobach, A. S.; Perov, A. A.; Rebrov, A. I.; Roshchupkina, O. S.; Tkacheva, V. A.; Stepanov, A. N. *Russ. Chem. Bull.* **1997**, *46*, 641.
- (4) Shigematsu, K.; Abe, K. *Chem. Express* **1992**, *7*, 905.
- (5) Darwish, A. D.; Abdul-Sada, A. K.; Langley, G. J.; Kroto, H. W.; Taylor, R.; Walton, D. R. M. *J. Chem. Soc., Perkin Trans. 2* **1995**, 2359.
- (6) Boltalina, O. V.; Bühl, M.; Khong, A.; Saunders, M. A.; Street, J. M.; Taylor, R. *J. Chem. Soc., Perkin Trans. 2* **1999**, 1475.
- (7) Rogner, I.; Birkett, P.; Campbell, E. E. B. *Int. J. Mass Spectrom. Ion Processes* **1996**, *156*, 103.
- (8) Vasil'ev, Y.; Wallis, D.; Nüchter, M.; Ondruschka, B.; Lobach, A.; Drewello, T. *Chem. Commun.* **2000**, 1233.
- (9) Vasil'ev, Y. V.; Boltalina, O. V.; Tuktarov, R. V.; Mazunov, V. A.; Sidorov, L. N. *Int. J. Mass Spectrom. Ion Processes* **1998**, *173*, 113.
- (10) Cozzolino, R.; Belgacem, O.; Drewello, T.; Käseberg, L.; Herzschuh, R.; Suslov, S.; Boltalina, O. V. *Eur. Mass Spectrom.* **1997**, *3*, 407.
- (11) Hettich, R. L.; Jin, C.; Britt, P. F.; Tuinman, A. A.; Compton, R. N. *Mater. Res. Soc. Symp. Proc.* **1994**, *349*, 133.
- (12) Zhou, L.; Tuinman, A. A.; Compton, R. N.; Lahamer, A. S. *Electrochem. Soc. Proc.* **1998**, *98*, 493.
- (13) Dunlap, B. I.; Brenner, D. W.; Schriver, G. W. *J. Phys. Chem.* **1994**, *98*, 1756.
- (14) Matsuzawa, N.; Fukunaga, T.; Dixon, D. A. *J. Phys. Chem.* **1992**, *96*, 10747.
- (15) Vasil'ev, Y. V.; Absalimov, R. R.; Lobach, A. S.; Nasibullaev, Sh. K.; Shul'ga, Y. M.; Mazunov, V. A. *Electrochem. Soc. Proc.* **1999**, *99*, 499.
- (16) Möder, M.; Nüchter, M.; Ondruschka, B.; Czira, G.; Vékey, K.; Barrow, M. P.; Drewello, T. *Int. J. Mass Spectrom. Ion Processes* **1999**, *196*, 599.
- (17) Clipston, N. L.; Brown, T.; Vasil'ev, Y. V.; Barrow, M. P.; Herzschuh, R.; Reuther, U.; Hirsch, A.; Drewello, T. *J. Phys. Chem. A* **2000**, *104*, 9171.
- (18) Taylor, R.; Barrow, M. P.; Drewello, T. *Chem. Commun.* **1998**, 2497.
- (19) Vasil'ev, Y. V.; Tuktarov, R. F.; Masunov, V. A. *Rapid. Commun. Mass Spectrom.* **1997**, *11*, 757.
- (20) Campbell, E. E. B.; Tellmann, R.; Rüchardt, C.; Gerst, M.; Ebenoch, J.; Beckhaus, H.-D. In *Physics and Chemistry of Fullerenes*; Prassides, K., Ed.; NATO ASI Series C; 1994; Vol. 443, p 27.
- (21) Banks, M. R.; Dale, M. J.; Gosney, I.; Hodgson, P. K. G.; Jennings, R. C. K.; Jones, A. C.; Lecoulre, J.; Langridge-Smith, P. R. R.; Maier, J. P.; Scrivens, J. H.; Smith, M. J. C.; Smyth, C. J.; Taylor, A. T.; Thorburn, P.; Webster, A. S. *J. Chem. Soc., Chem. Commun.* **1993**, 1149.
- (22) Jaffke, T.; Illenberger, E.; Lezius, M.; Matejcek, S.; Smith, D.; Märk, T. D. *Chem. Phys. Lett.* **1994**, *26*, 213.
- (23) Matejcek, S.; Märk, T. D.; Spanel, P.; Smith, D.; Jaffke, T.; Illenberger, E. *J. Chem. Phys.* **1995**, *102*, 2516.
- (24) Huang, J.; Carman, H. S., Jr.; Compton, R. N. *J. Phys. Chem.* **1995**, *99*, 1719.
- (25) Elhamidi, O.; Pommier, J.; Abouaf, R. *J. Phys. B: At. Mol. Opt. Phys.* **1997**, *30*, 4633.
- (26) Khvostenko, V. I.; Khvostenko, O. G.; Zikov, B. G.; Masunov, V. A. *Izvestiya AN SSSR, Ser. Khim. (Sov. Chem. Bull.)* **1977**, *3*, 717.
- (27) Compton, R. N.; Cooper, C. D. *J. Chem. Phys.* **1977**, *66*, 4325.
- (28) (a) Christophorou, L. G.; Carter, J. C.; Christodoulides, A. A. *Chem. Phys. Lett.* **1969**, *3*, 237. (b) Frey, W. F.; Compton, R. N.; Naff, W. T.; Schweinler, H. C. *Int. J. Mass Spectrom. Ion Phys.* **1973**, *12*, 19. (c) Cooper, C. D.; Frey, W. F.; Compton, R. N. *J. Chem. Phys.* **1978**, *69*, 2367. (d) Vasil'ev, Yu. V.; Mazunov, V. A.; Nazirov, E. R. *Org. Mass Spectrom.* **1991**, *26*, 739. (e) Palii, S. P.; Vasil'ev, Yu. V.; Asfandiarov, N. L.; Indrichan, K. M.; Gerbeleu, N. V.; Mazunov, V. A.; Dobrov, A. A. *Russ. J. Coord. Chem.* **1996**, *22*, 534. (f) Vasil'ev, Yu. V.; Zikov, B. G.; Fal'ko, V. S.; Lachinov, A. N.; Khvostenko, V. I.; Gileva, N. G. *Synth. Met.* **1997**, *84*, 975.
- (29) Wur, P.; Lykke, K. *J. Phys. Chem.* **1992**, *96*, 10129.
- (30) Darwish, A. D.; Avent, A. G.; Taylor, R.; Walton, D. R. M. *J. Chem. Soc., Perkin Trans. 2* **1996**, 2051.
- (31) Klots, C. E. *Chem. Phys. Lett.* **1991**, *186*, 73.
- (32) (a) Campbell, E. E. B.; Levine, R. D. *Comments At. Mol. Phys., Comments Mod. Phys.* **1999**, *1D*, 155. (b) Campbell, E. E. B.; Levine, R. D. *Annu. Rev. Phys. Chem.*, in press.
- (33) Vasil'ev, Y. V.; Absalimov, R. R.; Nasibullaev, Sh. K.; Lobach, A. S.; Drewello, T., manuscript in preparation.